Paleomagnetic definition of crustal fragmentation and Quaternary block rotations in the east Ventura Basin and San Fernando valley, southern California

Shaul Levi

College of Oceanographic and Atmospheric Sciences, Oregon State University, Corvallis, Oregon, USA

Robert S. Yeats

Department of Geosciences, Oregon State University, Corvallis, Oregon, USA

Received 25 February 2002; revised 8 May 2003; accepted 26 June 2003; published 30 October 2003.

[1] Paleomagnetic studies of the Pliocene-Quaternary Saugus Formation in the eastern part of the western Transverse Ranges of California show that the crust is fragmented into small domains, tens of kilometers in linear dimension, identified by rotation of reverse-fault blocks. In an area approximately 35 × 25 km in the San Fernando valley and east Ventura Basin we identified four distinct domains. Two domains, southwest of and adjacent to the San Gabriel fault, are rotated clockwise: (1) The Magic Mountain domain, R = 30° ± 5° and (2) the Merrick syncline domain, R = 34° ± 6°. The Magic Mountain domain has rotated since 1 Ma. Both rotated sections occur in hanging walls of active reverse faults, the Santa Susana and San Fernando faults, respectively. Structural data suggest that the fault tip of the Santa Susana fault is the rotation pivot of the Magic Mountain domain. Two additional blocks are unrotated: (1) the Van Norman Lake domain, directly south of the Santa Susana fault, and (2) the Soledad Canyon domain, immediately across the San Gabriel fault from the Magic Mountain domain, suggesting that the San Gabriel fault might be a domain boundary. Our results suggest that part of the clockwise rotation of some Miocene and older rocks in this area might have occurred in the Quaternary. The Plio-Pleistocene fragmentation and clockwise rotations continue at present, based on geodetic data, and represent crustal response to diffuse, oblique dextral shearing within the San Andreas fault system. *INDEX TERMS:* 1520 Geomagnetism and Paleomagnetism: Magnetostratigraphy; 1525 Geomagnetism and Paleomagnetism: Paleomagnetism applied to tectonics (regional, global); 8010 Structural Geology: Fractures and faults; 8110 Tectonophysics: Continental tectonics—general (0905); 9350 Information Related to Geographic Region: North America; *KEYWORDS:* block rotations, southern California, western Transverse Ranges, Saugus Formation, paleomagnetism, magnetostratigraphy. **Citation:** Levi, S., and R. S. Yeats, Paleomagnetic definition of crustal fragmentation and Quaternary block rotations in the east Ventura Basin and San Fernando valley, southern California, *Tectonics*, *22*(5), 1061, doi:10.1029/2002TC001377, 2003.

0278-7407/03/2002TC001377

1. Introduction

[2] In preplate tectonics days, *Cloos* [1955] reported on simple tabletop experiments, deforming soft clay cakes placed on a square of wire cloth. The fracture mosaic resulting from shear stress on the wet clay and comparisons with observed fault patterns of the San Andreas, Garlock and Big Pine fault system [*Hill and Dibblee*, 1953] led *Cloos* [1955, p. 255] to conclude: "...I think that the deformation might be clockwise by a couple whose directions would roughly parallel the San Andreas rift...." *Beck* [1976, 1980] recognized that most paleomagnetic results from the western edge of North America are discordant with respect to the stable craton, and the divergent directions usually have clockwise-rotated declinations and shallow inclinations, which might indicate northward transport. *Teissere and Beck* [1973] measured post-Cretaceous clockwise rotation of the Southern California batholith and pointed out that these observations are consistent with "transform faulting between the North American and Pacific plates."

[3] Geologists have long noted the east-west grain of the western Transverse Ranges (WTR) of southern California, which is oblique to the northwest trending Coast Ranges to the north and the Peninsular Ranges to the south. *Jones et al.* [1976] keyed on the general east-west trend of the slaty cleavage and fold axes of the Santa Monica Slate; they concluded that these Upper Jurassic rocks, together with the Santa Cruz Island Schist, "were disrupted and rotated in a clockwise direction." It is interesting that the same 1976 volume, where the Jones et al. article is published, also includes reports which cite geologic data to argue for counterclockwise rotations of the WTR as well as reports where rotations are not considered. The clockwise rotation of the WTR was not generally accepted until the paleomagnetic studies by Luyendyk and his students [*Kamerling and Luyendyk*, 1977, 1979, 1985; *Hornafius*, 1985; *Terres and Luyendyk*, 1985], who documented up to 90° clockwise rotation since early Miocene, continuing through the late

Cenozoic at an average rate of nearly 6°/m.y. [*Hornafius et al.*, 1986; *Liddicoat*, 1990; *Luyendyk*, 1991]. Further support for these results is provided by paleomagnetic studies of *Champion et al.* [1986], *Liddicoat* [1988], *Prothero and Britt* [1998], and *Prothero and Rapp* [2001]. Geodetic data suggest that these rotations are continuing at similar rates [*Jackson and Molnar*, 1990; *Donnellan et al.*, 1993; *Molnar and Gipson*, 1994].

[4] The consistent clockwise rotations measured in a variety of rocks of different ages over a broad geographical area of the WTR, its oblique structural grain and east-west faults, together with the absence of major subdividing north-south faults, led Luyendyk's group to envision the WTR as a series of individually rotating rigid panels with large aspect ratios, of the order of 100 km long and no more than a few tens of kilometers wide. The rotation is driven by dextral shear between two primary faults. Differential motion between panels is thought to be accommodated by left-lateral strike slip on block-bounding faults currently of east-west orientation. *Luyendyk* [1991] modified this model by introducing a component of extension across the trend of the deforming zone. *Crouch and Suppe* [1993] proposed that WTR rotation is associated with large-magnitude post-early Miocene extension of the Los Angeles Basin and inner California Borderland about a pivot now located near the northeastern corner of the province. Alternatively, the WTR rotation has been attributed to welding of the partially subducted Monterey microplate to the Pacific plate about 20 Ma [*Nicholson et al.*, 1994]. As the Pacific-Monterey spreading slowed and eventually ceased, the slip vector along the shallow northeast dipping subduction interface changed from slightly oblique subduction to transtensional dextral transform motion.

[5] *Whidden et al.* [1995] measured clockwise rotation in Eocene units between the Santa Ynez and Big Pine faults, and they argued that this area should be included in a northward expansion of the rotated WTR block. However, as indicated by *Beck* [1976, 1980], clockwise rotations are common for Cenozoic rocks in central and southern California, even in areas outside the WTR. Examples are: the Oligocene Morro Rock-Islay Hill igneous complex in San Luis Obispo County [*Greenhaus and Cox*, 1979]; the Miocene Monterey Formation at the Shell Beach section in the Pismo Basin [*Khan et al.*, 2001]; the upper Paleocene Pattiway Formation and the upper Oligocene-lower Miocene Soda Lake Shale Member of the Vaqueros Formation, Caliente Range in San Luis Obispo County [*Prothero and Hoffman*, 2001; *Prothero and Vacca*, 2001]; the Pliocene-Pleistocene Morales Formation in the Cuyama Basin [*Ellis et al.*, 1993]; and Pliocene-Pleistocene sediments from the Vallecito-Fish Creek area in the western Imperial valley [*Johnson et al.*, 1983].

[6] The observation that the angle of rotation within the WTR decreases eastward [*Terres and Luyendyk*, 1985; *Hornafius*, 1985], led *Dickinson* [1996] to propose an alternate geometrical model to explain the WTR rotations. He postulated diffuse northwest-southeast trending boundaries capable of differential rotations within panels. Hence while rotation is continuing in the western reaches of the WTR, rotation in the San Gabriel block, the area between the San Andreas and San Gabriel faults, ceased in the upper Miocene, about 9 Ma. Farther west in his Piru-Simi domain, rotation stopped about 5.2 Ma [*Dickinson*, 1996].

[7] Paleomagnetic studies of Plio-Pleistocene rocks in the Ventura Basin [*Levi et al.*, 1986; *Levi and Yeats*, 1993; *Liddicoat*, 1992, 2001a, 2001b] indicate more complex behavior in the eastern part of the WTR, unexplained by the above rotation models, which were developed mostly from measurements on Miocene and older rocks. First, the data indicate crustal fragmentation to smaller domains than the elongated panels in the models above. Second, rotation rates of Plio-Pleistocene strata can be much greater than those anticipated by models which consider high-aspect-ratio panels up to 100 km in length. Some domains have rotated in excess of 30° during the last million years, while other domains are unrotated.

[8] Here we report new results from the San Fernando valley and east Ventura Basin, west of the San Andreas fault in the Big Bend region between 34° and 35° north latitude, where the strike of the San Andreas fault is predominantly west-northwest, in contrast to its northwest trend north and south of the Big Bend (Figure 1). We studied four discrete sections of the late Cenozoic Saugus Formation in a relatively small area, about 35 × 25 km. The paleomagnetic results from two composite sections near the Magic Mountain Amusement Park and the Van Norman Lake reservoir were reported previously by *Levi and Yeats* [1993]. In this paper we present results from two additional composite sections: (1) Soledad Canyon in the city of Santa Clarita in the east Ventura Basin north of the San Gabriel fault, and (2) the Merrick syncline in the northern San Fernando valley (Figure 1). We also review other results from Plio-Pleistocene rocks farther west in the WTR [*Liddicoat*, 1992, 2001a, 2001b]. Overall, these data support crustal fragmentation and significant rotations of relatively small blocks with linear dimensions not exceeding 10–20 km. We try to account for the distribution of rotated and nonrotated sections in terms of mapped structural features. We also discuss the observed crustal fragmentation and rotations in a broader regional and temporal context.

2. Summary of the Geology of the Saugus Formation

[9] The continental and brackish water strata of the Saugus Formation [*Kew*, 1924; *Winterer and Durham*, 1962] occupy the center of the east Ventura Basin, where they are locally conformable with underlying Pliocene strata and are traversed by the San Gabriel fault. The Saugus is also found in the northern part of the San Fernando valley [*Oakeshott*, 1958; *Tsutsumi and Yeats*, 1999]. South of the Santa Susana fault, the Saugus occurs in discontinuous patches that unconformably overlie faulted strata as old as Eocene that are overridden by the Santa Susana fault [*Yeats*, 1987]. *Winterer and Durham* [1962] included in the Saugus brown, reddish brown, and tan sandstone and conglomerate, reddish brown mudstone,

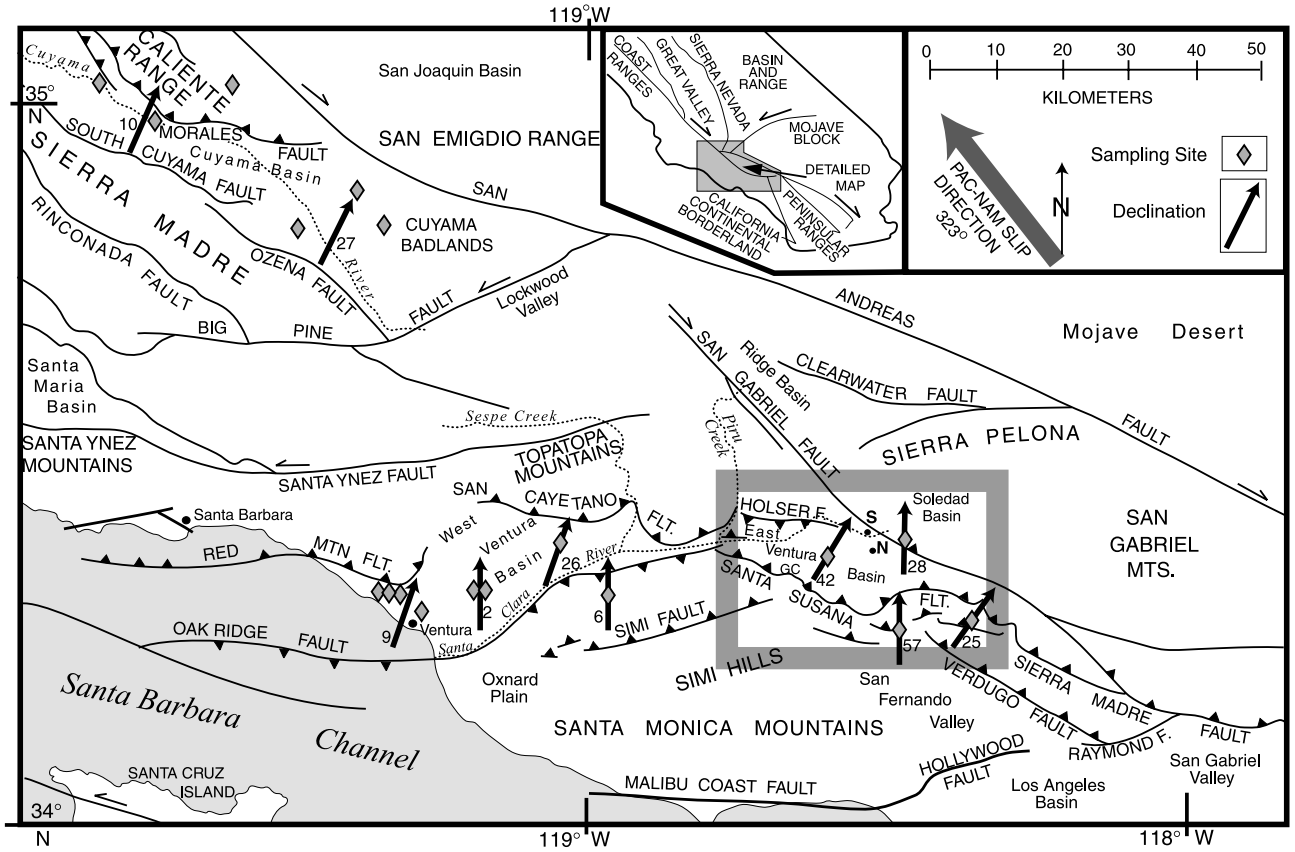

Figure 1. Index structural map of part of the California Transverse Ranges. The rectangle contains the area of this study, expanded in Figure 9, containing sites from *Levi and Yeats* [1993] and this study. Shaded diamonds identify locations of Plio-Pleistocene paleomagnetic results. Bold arrows through diamonds show average declination for individual studies; the numbers along arrows identify the number of sites associated with each declination. The data outside the rectangle in the west Ventura Basin are from *Liddicoat* [1992, 2001a, 2001b] and in the Cuyama Basin and Cuyama Badlands from *Ellis et al.* [1993]. GC, Gillibrand Canyon lateral ramp; N, Newhall; S, Saugus. The PAC-NAM plate vector is from *Atwater and Stock* [1998].

and greenish gray sandstone, all of which are deformed. The Saugus is overlain by generally flat-lying terrace deposits similar to, but somewhat more consolidated than, modern alluvium of the Santa Clara River.

3. Field and Laboratory Procedures

[10] Sites for paleomagnetic sampling were selected at the finer-grain sedimentary interbeds of mudstone, siltstone, sandy siltstone, and silty sandstone, typically 0.5 to 5 m thick, and generally sandwiched between much thicker beds of coarser-grain sandstone and conglomerate. At each site, digging was usually required to expose less weathered rock for sampling. The samples were oriented prior to their removal from the outcrop. Orientation was usually done by scribing a north arrow on a freshly carved and leveled horizontal surface. In this manner, we typically obtained three samples from each sedimentary layer. In the laboratory, each sample was releveled and cast in plaster of paris, and two specimens were cut or drilled from each hand sample for paleomagnetic measurements.

[11] *Levi and Yeats* [1993] showed, using both alternating fields (AF) and thermal demagnetization, that the fine-grain, younger, nonmarine Saugus strata usually retained a stable characteristic remanence. In contrast, older marine formations of late Tertiary age (Modelo, Towsley, and Fernando) were typically unstable and severely overprinted by the present field, and we were unsuccessful at isolating a characteristic remanence from even the fine-grain sites.

[12] For the Saugus Formation, thermal and AF demagnetization were, in general, equally effective at removing secondary overprints [*Levi and Yeats*, 1993]. AF demagnetization was chosen as the primary "cleaning" method for this study. At least two specimens from each site were demagnetized in progressively increasing AF up to between 40 and 100 mT (millitesla) to isolate the characteristic remanence and to determine the blanket AF for demagnetizing the remaining specimens at each site. At least four blanket AF levels were used to demagnetize each specimen of every site. *Levi and Yeats* [1993, Figures 5 and 6] present vector projection diagrams of AF and thermal demagneti-

Table 1. Paleomagnetism of the Kagel Ridge, Marek Canyon, and Little Tujunga Canyon Sites[a]

Site No.	*N/n*	D_R, deg	I_R, deg	*k*	α_{95}, deg	Demag Levels, mT	Bedding Strike, deg/Dip, deg
			Kagel Ridge Saugus Formation				
MC4	6/6		reverse				
MC3	6/6		reverse				276.0/61.0 N
MC2	6/6		reverse				
MC1	6/6		reverse				275.0/63.5 N
KR32	10/10	34	46	86	5	20–50	
KR31	6/6	240	−59	14	18	60–80	
KR30/31	6/6		reverse				
KR30	9/9	24	41	31	9	40–60	293.0/45.0 N
KR29	4/4		reverse				
KR28	5/5		reverse				
KR27	5/5	232	−49	46	11	40–60	
KR26	6/6	230	−50	42	10	60–100	
KR25/26	3/4	221	−59	39	20	40–80	
KR25	3/3	221	−49	43	19	60–100	299.0/48.5 N
KR24/25	4/4	237	−34	30	17	40–60	302.0/58.0 NE
KR24	5/5	220	−48	32	14	30–50	
KR23/24	4/4	230	−39	152	7	40–60	304.0/55.0 NE
KR23	6/6	231	−42	16	17	30–50	
KR22/23	5/9		reverse?				
KR22	7/10	29	43	17	15	30–50	
KR21/22	9/12	48	48	41	8	10–40	304.0/47.0 NE
KR21	8/9	31	46	19	13	20–50	
KR20	3/3	239	−44	68	15	20–40	290.0/49.0 N
KR19	3/4		reverse				293.0/50.0 N
KR18	2/4		reverse?				280.0/52.0 N
KR17	5/5		reverse				
KR16	3/5		reverse				
KR15	2/3		reverse				
KR14/15			indeterminate				
KR14	10/10	15	50	38	8	20–50	273.5/48.0 N
KR13			indeterminate				
KR12	7/10		reverse?				
KR11	6/6		reverse				280.0/46.5 N
KR10			indeterminate				
KR9	6/6	233	−42	35	12	60–100	280.0/54.0 N
			Fernando/Towsley Formation				
KR8	6/6		reverse				281.0/60.0 N
KR7	5/6		reverse				280.0/50.0 N
KR6	3/6		reverse?				250.0/45.0 N
KR5	4/6		reverse				280.0/46.0 N
KR4	2/4		reverse				279.0/46.0 N
KR3	4/4		reverse				266.0/48.0 N
KR2	3/6		reverse?				281.0/45.0 N
KR1			indeterminate				271.0/50.0 N
Mean (inverted to normal polarity)	**17**	**43**	**47**	**55**	**4.8**		
			Little Tujunga Canyon Saugus Formation				
LTC20			indeterminate				268.0/31.5 N
LTC21			indeterminate				227.0/25.0 N
LTC22	4/4	192	−48	21	21	30–80	
LTC23	6/6	185	−48	24	14	50–80	242.0/24.0 N
LTC24	5/6	190	−48	40	12	40–60	
LTC11	7/7	181	−66	73	7	30–80	116.5/29.0 S
LTC10	6/6	199	−31	102	7	40–60	120.0/32.0 S
LTC12	6/6		reverse				155.0/56.0 SW
LTC13	6/6		reverse?				151.0/59.0 SW
LTC14	4/6		reverse?				
LTC15	6/6	195	−33	119	6	50–80	
LTC6	6/6		reverse				275.0/63.5 N
LTC5	5/5		reverse				300.0/47.5 N
LTC4	4/6	192	−46	19	21	30–50	297.0/49.0 N
LTC3	6/6		reverse				
LTC2			indeterminate				
LTC1	5/6	205	−45	61	10	60–80	285.0/47.0 N
Mean	**8**	**193**	**−46**	**47**	**8**		
Mean (all sites as normal polarity)	**25**	**34**	**48**	**31**	**5**		

zation of individual Saugus specimens. Because this study is limited to the Saugus Formation, we do not present additional demagnetization diagrams in this paper, in an effort to conserve space. We refer the interested reader to *Levi and Yeats* [1993].

[13] Assessing the remanence stability of the Saugus sites was made easier by the predominance of reverse polarity, which is usually more readily distinguished from present-day overprints than normal polarity remanence. Many of the reverse specimens had a superimposed normal polarity component, which was usually removed by low-temperature (<200°C) thermal or low-field (<20 mT) AF demagnetization [*Levi and Yeats*, 1993]. Some of the reverse specimens showed a characteristic increase of the magnetization intensity during the initial stages of demagnetization. The characteristic paleomagnetic direction of each specimen was determined from 3 to 6 consecutive levels of progressive AF or thermal demagnetization.

[14] When appropriate, site mean directions were calculated in two ways. First, each specimen was assigned equal weight; on average, this resulted in data from two specimens per oriented hand sample and six specimens per site. Second, we combined the data of specimens from each oriented sample, thereby halving the number of independent vectors. The two methods yielded essentially identical directions. For most sites, estimates of the *Fisher* [1953] precision parameter (k) increased significantly or hardly changed when the number of independent measurements was halved, while the radius of the 95% cone of confidence (α_{95}) increased or remained the same. Site mean paleomagnetic directions and the associated statistical parameters (k and α_{95}) for the Saugus Formation in the Merrick syncline and Soledad Canyon are listed in Tables 1 and 2, where each specimen is assigned unit weight. In Merrick syncline, all 25 sites that yielded directions have $\alpha_{95} \leq 21°$. Of the 27 sites with paleomagnetic directions at Soledad Canyon, 25 have $\alpha_{95} \leq 20°$; the remaining 2 sites have α_{95} values of 22° and 30°. A further indication of the high data quality is seen in the N/n columns of the tables, where only relatively few specimens were rejected based on their demagnetization behavior.

[15] While we were not able to do a formal fold test, the steep dips of the sampled Saugus sections (Figures 2 and 4; Tables 1 and 2) were suitable for a pseudo- or partial-fold test. We observed that the structurally uncorrected, in situ, directions have no meaning when compared with the known Neogene direction in this area, whereas the structurally corrected directions are consistent with the Neogene geomagnetic field [*Levi and Yeats*, 1993], suggesting that the remanence predates folding. The presence of normal polarity sites at the four Saugus sections suggests that each section spans sufficient time to average secular variations.

4. Results and Discussion

4.1. Magnetostratigraphy and Age of the Saugus Formation

[16] Previous results from a Saugus reference section along the Santa Clara River and along an electric transmission line south of the Magic Mountain amusement park show that the Saugus was deposited between 2.3 and 0.4 Ma, based on the discovery of the 0.76 Ma Bishop ash (A.M. Sarna-Wojcicki in the work of *Levi et al.* [1986]) and the pattern of paleomagnetic polarity reversals in the Magic Mountain composite section. In the northern San Fernando valley just south of the Santa Susana fault in the Van Norman Lake section, the Saugus strata span a similar time interval as in the Magic Mountain area. In both sections, Saugus deposition was sufficiently protracted and is represented by sufficient magnetostratigraphic detail to estimate the average sedimentation rates: 0.9 km/m.y. in the Magic Mountain section and 1.1 km/m.y. in the Van Norman Lake section [*Levi and Yeats*, 1993].

[17] In the Merrick syncline, the Saugus and underlying Fernando and/or Towsley strata were sampled along the Kagel Ridge firebreak, along Little Tujunga Canyon, and in Marek Canyon (Figure 2), totaling 60 sedimentary beds (sites), and representing a stratigraphic thickness of approximately 1300 m. Fifty-two of these sites gave polarity information, of which 25 beds yielded paleomagnetic directions. Forty-six of the 52 sites that retained polarity information are reverse. Along the Kagel Ridge firebreak, the lowest eight sites from the lowermost 200 m are mapped as the Fernando and/or Towsley Formation [*Barrows et al.*, 1975], and the six sites within this formation that retained polarity information are all reverse. The four uppermost Saugus sites in this composite section are on the west side of Marek Canyon, closest to the axis of the Merrick syncline, and they all have reverse polarity. Along Little Tujunga Canyon, 14 of 17 sites retained magnetic polarity; they are all reverse. The predominance of reverse polarity and analogy with the Saugus in the Magic Mountain reference section strongly suggest that the sediments in the Merrick syncline composite section were deposited during the Matuyama chron, 0.78–2.60 Ma.

[18] Among the 39 sites sampled along the Kagel Ridge firebreak (east of Kagel Canyon), six have normal polarity, representing four normal polarity intervals (Figure 3). All six normal sites yielded paleomagnetic directions with respectable precision parameters (Table 1), contributing to

Note to Table 1

[a]To the degree possible, sites are listed in stratigraphic sequence, with the youngest sites at the top and oldest at the bottom. *N*/*n*, number of specimens used in calculations/number of specimens measured; D_R, I_R, structurally corrected declination (D) and inclination (I), rotated to horizontal using measured bedding attitude (strike/dip); *k*, best estimate of precision parameter of Fisher distribution; α_{95}, radius in degrees of the 95% cone of confidence about the mean direction; demag levels (mT), range of consecutive AF demagnetization steps in millitesla used for obtaining the stable direction of each specimen. Site location is 34.30°N, 241.64°E.

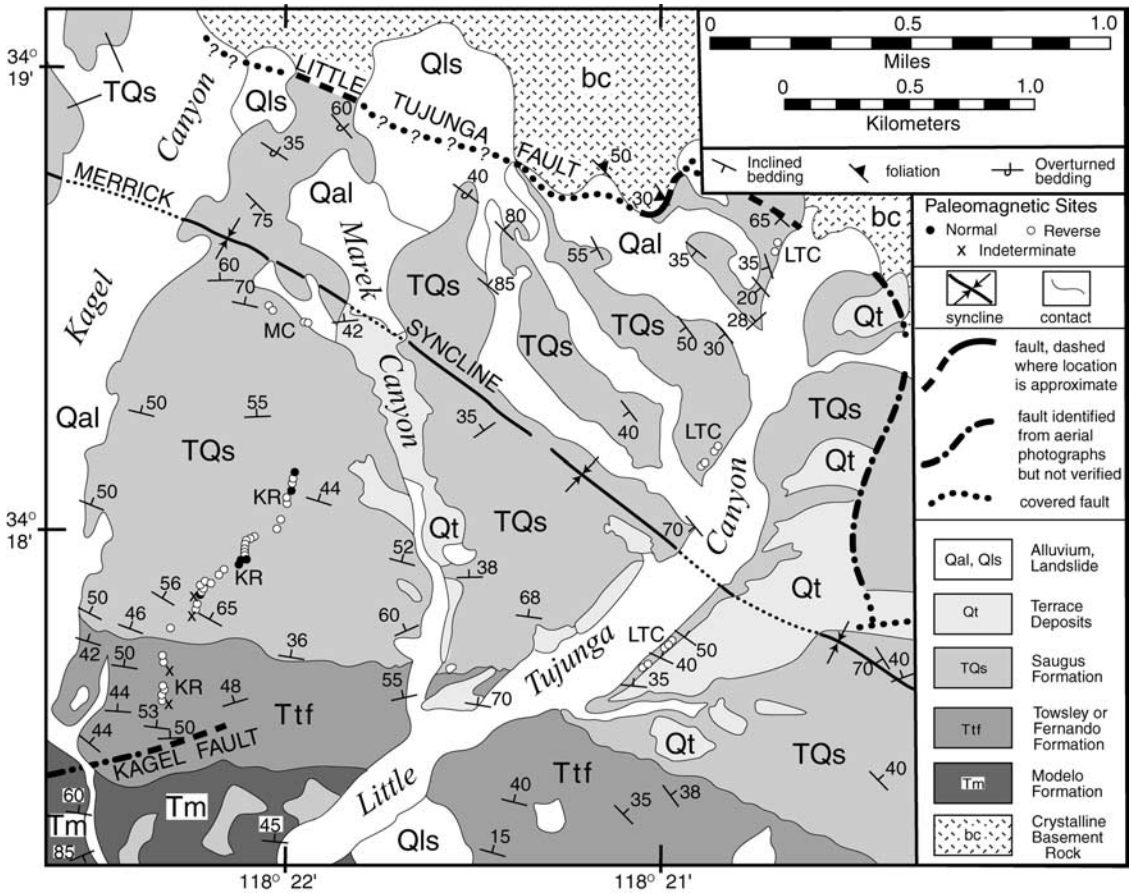

Figure 2. Location of paleomagnetic sites in the Merrick syncline domain at the northern edge of the San Fernando valley. KR, Kagel Ridge; LTC, Little Tujunga Canyon; MC, Marek Canyon. Open circles indicate reverse polarity; solid circles indicate normal polarity. Paleomagnetic data are listed in Table 1. Geologic map is from *Barrows et al.* [1975].

our confidence in identifying them as normal. Only one of the normal intervals is represented by more than a single site. Although it is not common to measure four Matuyama subchrons in a single section of continental sediments, all six normal sites are from the Kagel Ridge section (Figure 2), so unrecognized double sampling of the same sedimentary bed is unlikely.

[19] The Matuyama reverse chron might include six, and possibly more, normal subchrons: Jaramillo (0.99–1.05 Ma), Cobb Mountain (1.18 Ma), Gilsa (1.7 Ma ?), Olduvai (1.78–1.96 Ma), Reunion II (2.11–2.15 Ma), and Reunion I (2.19–2.27 Ma) [e.g., *Singer et al.*, 1999; *McDougall*, 1979; *McDougall et al.*, 1992]. It is not possible to uniquely correlate the short intervals of normal polarity measured in the Kagel Ridge section with specific Matuyama subchrons, and none of the possible correlations below is entirely satisfactory. The most frequently observed subchrons in the Matuyama are the Olduvai and the Jaramillo. One possible correlation is that the normal intervals represent (from top to bottom) the Jaramillo, Cobb Mountain, Olduvai, and one of the Reunion subchrons. The attraction of this correlation is that it includes the two longest subchrons in the Matuyama. The least appealing part of this correlation is the rather extensive reverse section overlying the Jaramillo (Figure 3), which would require higher sedimentation rates in the younger part of the section. It is also possible to correlate the four normal intervals with the Cobb Mountain, Gilsa, Olduvai and one of the Reunion subchrons. On the positive side, this scheme correlates the Olduvai with the most robust normal interval observed in the section. On the other hand, the Gilsa subchron is rarely observed in continental sediments. Alternatively, the normal intervals in the section might represent the Gilsa, Olduvai, and two Reunion subchrons. In this correlation, the longest normal interval in the section is associated with the younger Reunion subchron, which is considered to have shorter duration than either the Olduvai or the older Reunion subchron. Support for this interpretation is found in the relative spacings of the normal intervals, which is more similar to the recognized polarity time scale, assuming uniform deposition rates. The calculated sedimentation rates increase progressively from 0.38 km/Ma for the first interpretation to 0.90 km/Ma for the third; the latter value is similar to the average sedimentation rates for the

Table 2. Soledad Canyon: Summary of Paleomagnetic Results[a]

Site No.	*N*/*n*	D_R, deg	I_R, deg	*k*	α_{95}, deg	Demag Levels, mT	Bedding Strike, deg/Dip, deg
SOC15	6/6	190.2	−18.2	37	11	60–80 (2)	106.5/44.5 S
SOC14	6/6	176.7	−47.0	128	6	50–80 (3)	125/59 SW
SOC13	4/6	169.1	−37.5	50	13	40–80 (4)	117/32 S
SOC12	6/6	174.9	−48.6	113	6	50–80 (3)	
SOC11	6/6	145.9	−52.2	406	3	50–80 (3)	119/57.5 S
SOC10	6/6	173.1	−58.9	66	8	50–80 (3)	127/57 SW
SOC9	6/6	194.3	−46.3	241	4	40–80 (4)	124/58 SW
SOC8	4/6	32.5	71.9	33	16	40–100 (5)	114/58.5 S
SOC6	6/6	33.3	43.8	50	10	20–50 (4)	
SOC5	6/6	150.1	−30.9	16	18	50–100 (4)	94.5/36 S
SOC4	5/6	25.5	46.3	19	18	50–100 (4)	91.5/49.5 S
SOC3	6/6	39.1	59.4	87	7	50–80 (3)	99/54 S
SOC2	6/6	186.5	−50.5	62	9	30–60 (4)	
SOC1	6/6	177.3	−48.7	106	6	30–50 (3)	78/53 S
SO38	6/6	176.8	−41.7	49	10	30–80 (5)	160/37 SW
SO34	6/8	178.7	−42.8	43	10	30–60 (4)	150/30 SW
SO32	6/6		indeterminate				163/34 SW
SO30	3/6	179.6	−44.7	18	30	50–80 (3)	154/39.5 SW
SO28	6/6		reverse				150/35 SW
SO26	6/6	160.6	−55.1	226	5	10–50 (5)	148/34 SW
SO24	6/6	165.5	−43.3	48	10	10–50 (5)	162/28 SW
SO20	6/6	173.4	−53.1	150	5	20–80 (6)	149/25 SW
SO78	4/6		reverse				151/42 SW
SO76			normal?				179/37 W
SO74	4/6	199.7	−39.2	18	22	40–80 (4)	155/35 SW
SO70	6/6	180.4	−56.4	104	7	20–80 (6)	144/26 SW
SO66	6/6	177.6	−37.8	679	3	20–80 (6)	159/29 SW
SO64	6/6	167.6	−40.9	480	3	30–80 (5)	152/26 SW
SO60	6/6	163.6	−43.6	74	8	30–60 (4)	155/36 SW
SO58	4/6	188.3	−41.9	33	16	10–50 (5)	178/26 W
SO56	3/6	196.5	−44.6	433	6	20–60 (5)	
SO54	6/6	181.0	−36.7	99	7	20–80 (6)	157/16 SW
SO52			normal?				
SO50			normal?				138/18 SW
Mean (all sites as normal polarity)	**27**	**0**	**48.1**	**31**	**5.1**		
Mean (reverse sites)	**23**	**176**	**−46.1**	**49**	**4.4**		
Mean (normal sites)	**4**	**31**	**55**	**37**	**15.3**		

[a]See Table 1 for definitions and descriptions of column headings. Site location is 31.42°N, 241.48°E.

sections near Magic Mountain and Van Norman Lake, which might be considered additional support for the third interpretation. More information is required to further constrain and select from among these interpretations.

[20] In the San Gabriel block, just northeast of the San Gabriel fault in the city of Santa Clarita, the Saugus was sampled south of Soledad Canyon near its type locality. Fourteen Saugus sites (SOC 1–15) were sampled at the western end of Soledad Canyon along the Southern Pacific Railroad tracks, east of Bouquet Junction and south of Soledad Canyon Road (Figure 4). The sedimentary beds have southerly dips 35°–60°, striking 78°–125° [*Winterer and Durham*, 1962; *Dibblee*, 1996]. These sites are distributed along approximately 1 km of the east-southeast trending railroad tracks, representing a stratigraphic section of the order of 0.5 km in thickness. Twenty additional sites (SO 20–78) were sampled immediately east-southeast of the 14 mentioned above, and they, too, have consistent bedding attitudes with an average strike of about 155° and southwesterly dips of about 30°.

[21] All 34 sites are in the San Gabriel block, and they are all within 0.5 km of the San Gabriel fault. From 33 of the sites, paleomagnetic polarity was recovered, and 28 sites yielded complete paleomagnetic directions; results from one site were indeterminate. The normal polarity determinations of sites SO 50, 52 and 76 (Table 2) are questionable, because they are based on thermal demagnetization of a single specimen at each site, analyzed after the AF demagnetization results were unsuccessful. Sites SOC 1–15 are in stratigraphic sequence with site 1 the oldest and site 15 (nearest to Bouquet Junction) the most recent. Sites SO 20–78 are also listed in stratigraphic order with site SO 50 the oldest to site SO 38 the youngest (Table 2). Because these two subsections were deformed with different bedding attitudes, their stratigraphic relationships are insufficient for assembling a composite stratigraphic column (Figure 5). On the basis of the predominantly reverse polarity of these sections and by analogy with the Saugus reference section near Magic Mountain, we conclude that the sampled Saugus sites in Soledad Canyon were also deposited during the Matuyama chron, 0.78–2.60 Ma. The normal sites represent at least two and possibly as many as four normal polarity subchrons. However, it is not known at present which of

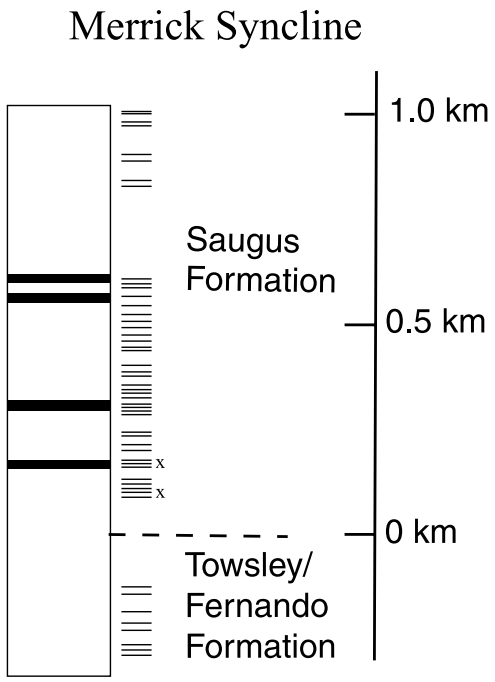

Figure 3. Magnetic polarity stratigraphy of the composite Merrick syncline section (KR, LTC, and MC) at the northern edge of the San Fernando valley. Black is normal polarity; white is reverse polarity. Horizontal dashes to the right of the polarity column represent sampling sites; crosses next to dashes indicate sites with indeterminate polarity. Depth scale on the right-hand side shows stratigraphic thickness.

the Matuyama subchrons are represented by these normal units (Figure 6).

4.2. Domain Rotations and Crustal Fragmentation

[22] Our study in the east Ventura Basin and San Fernando valley focuses on four sections of a single formation in a small area about 35 × 25 km (Figure 1). In addition, the Saugus Formation is comparatively young; it was deposited between 2.3 and 0.4 Ma. Each of the sampled Saugus sections includes both normal and reverse polarity sites, suggesting that sufficient time is represented by each section to average secular variation. Therefore our study is suitable for exploring relatively short wavelength tectonic movements in this region of southern California since Saugus deposition. Because of the Plio-Pleistocene age of the Saugus Formation, tectonic movements are judged with respect to the present geocentric axial dipole direction at the sampling sites: declination, $D = 0°$; inclination, $I = 54°$; and rotation $R = D$. The uncertainties in rotation ΔR are calculated following *Demarest* [1983]. Recent plate circuit calculations [*Atwater and Stock*, 1998] show that since 8 Ma the average displacement of the Pacific plate relative to stable North America has been ~52 mm/yr along azimuth 323°. Therefore north-south transport within the San Andreas shear zone has not exceeded 100 km since Saugus deposition, which cannot be resolved by paleomagnetism.

[23] The continental Saugus has sufficiently stable remanence that complete paleomagnetic directions were recovered from a majority of the sampled sites. In the Magic Mountain area, 42 of 70 sites yielded directions, and more than 90% of the specimens from sites with directions were used in the calculations. The 29 Saugus Matuyama sites show clockwise rotation $R = 30° \pm 5°$ since about 2.3 Ma. Because there is no apparent trend in the declinations of the Saugus Matuyama sites with stratigraphic position, rotation of these sediments began less than one million years ago. The ten Brunhes sites are rotated clockwise $R = 14° \pm 6°$. (Three sites are considered to have acquired their remanence during a polarity transition.) In the Van Norman Lake and Horse Flats areas south of the Santa Susana fault, more than two thirds of the sites gave directions. The mean declination for 57 sites is $D = 360° \pm 4°$, showing no evidence for rotation [*Levi and Yeats*, 1993].

[24] In the Merrick syncline area (Table 1, Figure 7), 25 of 52 Saugus sites yielded paleomagnetic directions. The mean paleomagnetic direction for the 25 sites is $D = 34°$, $I = 48°$. The mean declination indicates clockwise rotation $R = 34° \pm 6°$ about a vertical axis after this sequence of Saugus was deposited. The mean inclination is 6° shallower than expected from a geocentric axial dipole at this location, behavior not uncommon for continental sediments.

[25] In Soledad Canyon (Table 2, Figure 8), paleomagnetic directions were recovered from 28 of 34 Saugus sites. The average direction of the four normal sites (not sufficient to average secular variation) is 31°. They were combined with the 23 reverse sites to obtain the mean direction for the Soledad Canyon domain: $D = 0.4°$, $I = 48°$; $\Delta R = 6°$. Again, there is evidence for 6° inclination shallowing, but there is no evidence for rotation of this segment of the San Gabriel block just northeast of the San Gabriel fault since the deposition of the Saugus Formation.

[26] The Saugus paleomagnetic results indicate a more intricate tectonic pattern in the east Ventura Basin and San Fernando valley than suggested by earlier models for WTR tectonics. The relatively small study area is subdivided into at least four more or less equidimensional domains, whose lengths are of the order of 10–20 km (Figure 9). These domains are considerably smaller than the long panels in the western parts of the WTR [e.g., *Luyendyk*, 1991]. The average rotation is clockwise, as expected in a regime of dextral shear. However, two of the domains are unrotated. The other two domains have rotated clockwise 30° and 34° since the beginning of Saugus deposition, ~2.3 Ma. The rotation of the Magic Mountain domain is constrained to be younger than 1 Ma. In the next section we discuss the fragmented crustal blocks in context of mapped structural features.

[27] Paleomagnetic studies by *Liddicoat* [1992, 2001a, 2001b] of the Pliocene and early Pleistocene Fernando Formation directly west of our study area (Figure 1) are consistent with our observations. Six sites at Balcom Canyon, south of the Oak Ridge fault, show no significant

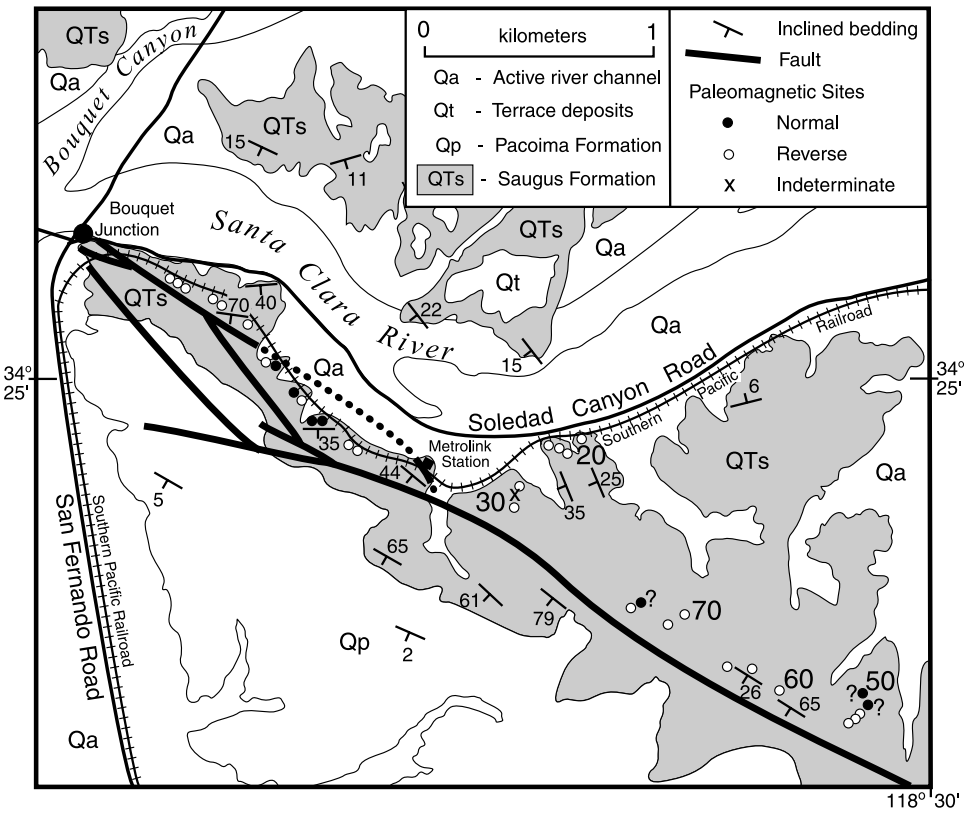

Figure 4. Location of paleomagnetic sites south of the Soledad Canyon Road. Open circles indicate reverse polarity; solid circles indicate normal polarity. The SOC sites are along railroad tracks between Metrolink station and Bouquet Junction. The SO sites are along railroad tracks east of Metrolink station and on ridge to the south. Large numerals (20, 30, 50, 60, and 70) identify enough site numbers to allow location of all SO sites. Paleomagnetic data are listed in Table 2. Geologic map is modified slightly from *Winterer and Durham* [1962] and *Dibblee* [1996]; faults are from *Swanson* [2001].

rotation (6° counterclockwise [*Liddicoat*, 2001a]). At Santa Paula Creek, about 10 km northwest of Balcom Canyon, 26 sites indicate clockwise rotation of 20° ± 9° [*Liddicoat*, 1992]. At Aliso and Wheeler canyons northeast of Ventura, the average declination of two reverse sites points south, while nine sites in the Ventura Avenue anticline near the coast are rotated 20° clockwise (Figure 1) [*Liddicoat*, 2001b]. These data suggest that the crust of this part of the Western Transverse Ranges has fragmented into smaller and more equidimensional blocks than previously recognized for this region.

[28] The Plio-Pleistocene Saugus and Fernando formations are younger than other units whose paleomagnetism has been studied in this area. The cumulative tectonic signature recorded in the older rocks might include an imprint imposed during the Quaternary. However, barring independent data, it is rare to be able to resolve the detailed timing of the later tectonic events, and conclusions are generally stated with respect to the age of the rocks (e.g., post-Eocene, post-Miocene, etc.). Results from the Pliocene-Pleistocene Saugus and Fernando formations provide the youngest data on WTR fragmentation and rotations available to date, which probably affected at least some of the older rocks in the region.

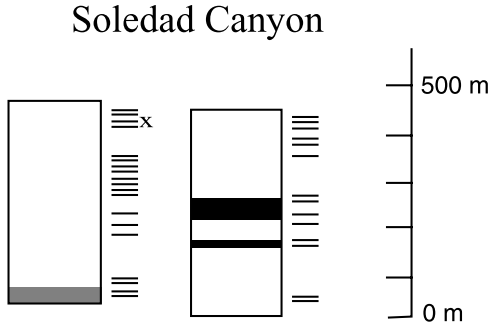

Figure 5. Magnetic polarity stratigraphy of the composite Soledad Canyon sites: SOC (right) and SO (left). Black indicates normal polarity, white indicates reverse polarity, and shaded indicates questionable polarity. Horizontal dashes to the right of the polarity columns represent sampling sites; crosses next to dashes indicate sites with indeterminate polarity. The depth scale on the right-hand side shows stratigraphic thickness.

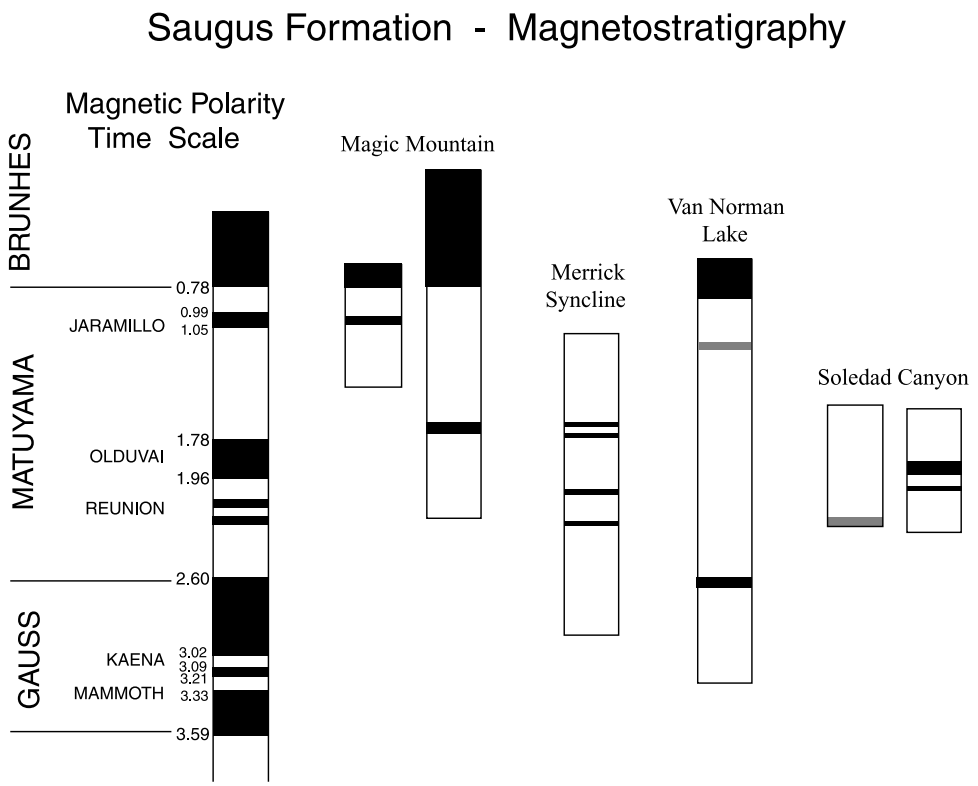

Figure 6. Magnetic polarity stratigraphy of the four composite Saugus sections, Magic Mountain, Merrick syncline, Van Norman Lake, and Soledad Canyon, along with the magnetic polarity time scale. Black indicates normal polarity, white indicates reverse polarity, and gray indicates questionable polarity.

[29] The tectonics recorded by the Fernando and Saugus formations occurred well after the migration of the Pacific-North America plate boundary, about 6–4 Ma, to its present site in the Gulf of California [*Ness et al.*, 1991; *Lonsdale*, 1991], extending northwestward through the Salton Trough, and connecting with the present trace of the San Andreas fault. In this regard, the Plio-Pleistocene movements are somewhat different from earlier Miocene tectonics of the WTR, which occurred while the plate boundary was west of Baja California along the California continental borderland or at the base of the continental slope. In the early and middle Miocene, the Farallon-Pacific-North America plate interactions were in transition from oblique subduction [e.g., *Nicholson et al.*, 1994] with a significant component of crustal extension [e.g., *Crouch and Suppe*, 1993] to the current regime of dextral strike slip. Late Cenozoic plate interactions in this area of southern California have consistently included a component of dextral shear, implying that, on average, clockwise rotations are favored, although an occasional counterclockwise-rotated domain may be observed, and some blocks may be unrotated. The magnitudes and sense of domain rotations depend on factors including their sizes, shapes, and interactions along boundaries with neighboring domains and adjacent structural elements.

[30] In the Big Bend region, the strike of the San Andreas fault is approximately 295° [*Jackson and Molnar*, 1990], while the direction of relative plate motion is 323° [*Atwater and Stock*, 1998] (Figure 1). Therefore in the sampling area, there is a significant component of motion normal to the San Andreas fault. This leads to comparatively greater compressive strain across the plates than elsewhere along the fault, with significant crustal shortening and uplift, accompanied by folding and thrusting. We suggest that these enhanced interactions amplify crustal fragmentation, leading to smaller domains in the eastern WTR, while toward the coast, further removed from the San Andreas fault, the WTR crust is bounded by east-west faults into larger blocks with high aspect ratios [*Luyendyk et al.*, 1985; *Jackson and Molnar*, 1990; *Luyendyk*, 1991]. By analogy, northwest and southeast of the Big Bend, where plate interactions are less oblique, diffuse dextral shearing might lead to less intense crustal fragmentation and rotations, and rotations might more frequently occur in extensional settings of pull-apart basins, as documented and discussed by *Greenhaus and Cox* [1979].

[31] The net clockwise rotation of the four sections in the sampled area is consistent with dextral shearing and oblique convergence between the Pacific and North America plates. We note that the two rotated domains are southwest of and adjacent to the San Gabriel fault. This might suggest that the San Gabriel fault serves as a boundary and/or pivot for domain rotations, although it has experienced only minor strike slip movement since Saugus deposition [*Yeats et al.*, 1994; *Yeats and Stitt*, 2003]. The paleomagnetic results from Pliocene and Pleistocene formations in the WTR show

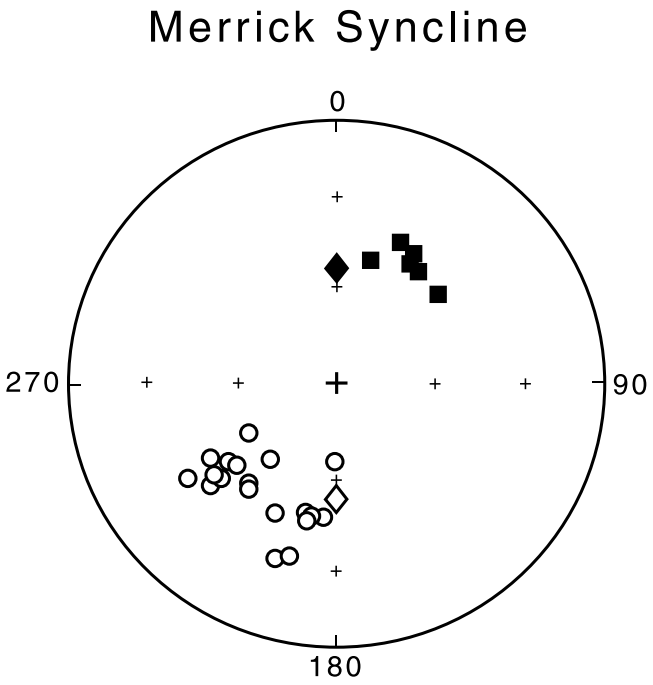

Figure 7. Site mean, structurally corrected paleomagnetic directions for the Merrick syncline domain. Diamonds represent normal (solid) and reverse (open) directions of the Plio-Pleistocene geocentric axial dipole. Open circles are reverse upper hemisphere directions of Matuyama sites; solid squares represent normal polarity Matuyama sites. The perimeter circle indicates horizontal directions; interior crosses designate 30° increments of inclination.

that significant rotation has occurred during the last few million years, including the Brunhes chron since 0.8 million years. Clockwise rotations in this region are continuing to this day and are an integral part of the present regime of active tectonics [*Jackson and Molnar*, 1990; *Donnellan et al.*, 1993; *Molnar and Gipson*, 1994].

4.3. Block Rotations in Context of Mapped Structural Features

[32] Both rotated sections occur in hanging walls of active reverse faults in the western Transverse Ranges (Figure 9 [*Yeats*, 1987; *Yeats et al.*, 1994]): the Santa Susana and San Fernando faults, with a regional strike WNW-ESE. The Santa Susana fault contains two northeast trending, left-stepping lateral ramps, the Gillibrand Canyon ramp (GC) on the west and the San Fernando ramp (SF, also called the Chatsworth ramp) on the east, at the western edge of the San Fernando valley (Figure 10) [*Yeats*, 1987]. The main shock and many aftershocks of the 1971 Sylmar (San Fernando) earthquake followed the San Fernando ramp, many with left-lateral fault plane solutions [*Whitcomb et al.*, 1973]. At Aliso Canyon Oil Field immediately west of SF, dip slip on the Santa Susana fault is 4.9–5.9 km based on a retrodeformable cross section [*Huftile and Yeats*, 1996, Table 1], whereas no dip slip was measured at the Santa Susana fault tip 10 km west of the GC [*Ricketts and Whaley*, 1975; *Yeats*, 1987]. This observation might be interpreted as clockwise rotation of the hanging wall of the Santa Susana fault with respect to its footwall, with a pivot at the fault tip, T (Figure 10). Rotation by 30° of a rigid plate 27.5 km long, the distance between T and SF (Figure 10), produces total slip of 14 km, which is much greater than the dip slip measured in the Aliso Canyon Oil Field cross section.

[33] An alternative model is that clockwise rotation occurs in two segments: the Newhall-Potrero and Placerita segments of *Yeats et al.* [1994], separated by the Gillibrand Canyon lateral ramp (GC). The northeast trending segment boundary is not a through-going surface fault, but it separates contrasting structures west and east of it: the Newhall-Potrero anticline and Del Valle fault to the west and the Pico anticline and adjacent syncline to the east [*Yeats*, 1987, Figure 9.9]. A 30° rotation of the 10 km long Newhall-Potrero segment, pivoting at the fault tip, results in a total slip of 5 km at GC. The length of the GC lateral step, as measured by stepped-left structure contours on the Santa Susana fault [*Yeats*, 1987, Figure 9.8], is 2 km. The left separation of the pre-Saugus Torrey fault in the footwall of the Santa Susana fault is slightly greater than 4 km [*Yeats*, 1987, Figure 9.6]. Additional shortening in the hanging wall takes place by strong folding, locally overturned, west of

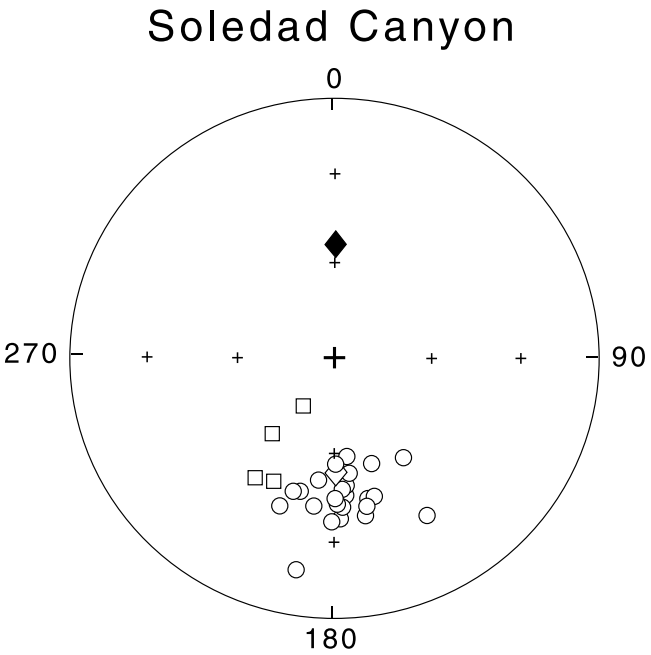

Figure 8. Site mean, structurally corrected paleomagnetic directions for the Soledad Canyon domain. Diamonds represent normal and reverse directions of the Plio-Pleistocene geocentric axial dipole. Open circles are upper hemisphere directions of Matuyama sites; open squares represent normal polarity Matuyama sites inverted through the origin to reverse polarity. The perimeter circle indicates horizontal directions; interior crosses designate 30° increments of inclination.

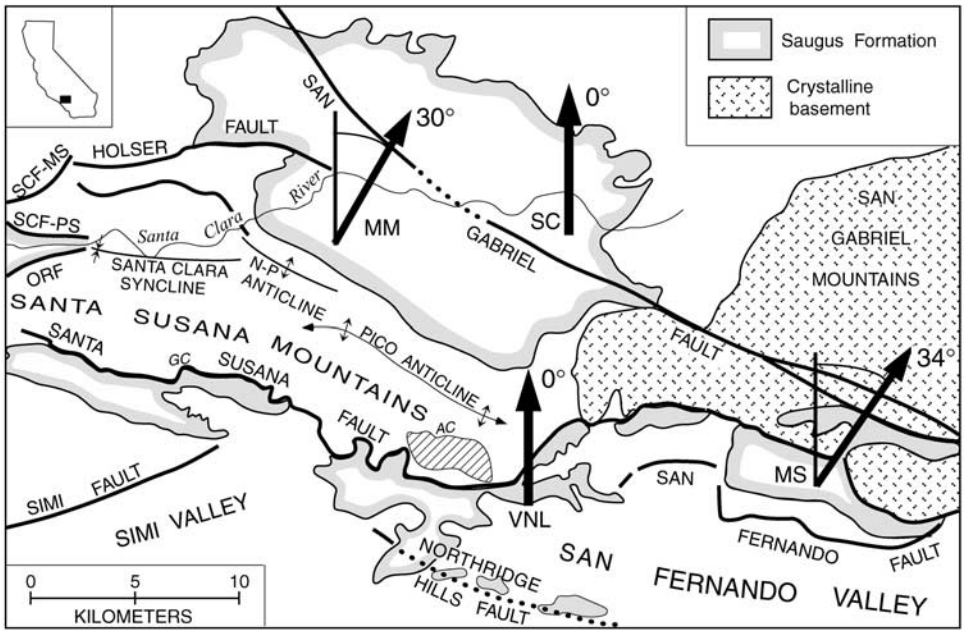

Figure 9. Tectonic map of the four study areas described by *Levi and Yeats* [1993] and this paper. MS, Merrick syncline domain: Kagel Ridge, Little Tujunga Canyon, and Marek Canyon sections; SC, Soledad Canyon; MM, Transmission Line and Santa Clara River sections of the Magic Mountain area; VNL, Van Norman Lake and Horse Flats sections in the San Fernando valley. Bold arrows indicate the average declination of each area with associated magnitude of clockwise rotation. Faults are shown in heavy lines and dotted lines where covered. ORF, Oak Ridge fault; SCF-MS, San Cayetano fault, Main strand; SCF-PS, San Cayetano fault, Piru strand; AC, Aliso Canyon Oil Field; GC, Gillibrand Canyon lateral ramp; N-P, Newhall-Potrero anticline.

GC that is not present east of GC (Figure 10 [*Yeats*, 1987, Figures 9.2 and 9.9]).

[34] At present there are no paleomagnetic data to test the rotation of the Placerita segment. A pivot point for this block is assumed in the vicinity of Gillibrand Canyon. If the hanging wall block between GC and SF rotated as a rigid block, rotation of the order of 10° to 15° would be required to account for the 4.1 km shortening calculated by *Huftile and Yeats* [1996, Table 1] . The strike of the Santa Susana fault east of GC changes from east-southeast to east-west at point Y (Figure 10) just west of the Aliso Canyon oilfield [*Yeats*, 1987, Figure 9.8], such that the rotation of the Placerita block might be limited to the hanging wall block between GC and Y.

[35] The nonrotated Van Norman Lake section is in the footwall of the Santa Susana fault; it is also in the hanging wall of the Mission Hills reverse fault (Figure 11 [*Tsutsumi and Yeats*, 1999]). The Mission Hills fault strikes east-west, whereas, over most of its length, the Santa Susana fault strikes WNW-ESE, at an angle of about 30° with respect to the strike of the Mission Hills fault and 30° with respect to the strike of the Santa Susana fault between Y and SF. The inference is that whereas the WNW-ESE Santa Susana fault is rotated, the E–W Mission Hills fault is not. We propose that the nonrotated Van Norman Lake domain is related to the nonrotated Mission Hills fault.

[36] We suggest that the rotation of the Merrick syncline domain might be limited to the 10 km long San Fernando fault that ruptured in 1971 (Figure 11). The Merrick syncline domain is on the flanks of the east-southeast trending Merrick syncline (MS, Figure 11), bounded on the west by a segment boundary at Pacoima Wash and on the east by a segment boundary at Big Tujunga Canyon north of Sunland, the eastern terminus of the 1971 surface rupture (S, Figure 11). We propose that the pivot for the rotation of the Merrick syncline domain is in the northeast trending Pacoima Wash segment boundary of *Tsutsumi and Yeats* [1999, Figure 8] . Across this segment boundary, the change of strike between the 1971 San Fernando fault and the Sylmar-Mission Wells fault [*Sharp*, 1975] and between the Merrick syncline and Mission Hills syncline is approximately the same as the difference between the rotated Merrick syncline domain to the east and the unrotated Van Norman Lake domain to the west (Figure 11). This rotation boundary may be analogous to the diffuse "knee joint" boundaries of *Dickinson* [1996] to explain the difference in rotation within "rigid" panels of the WTR. A 34° rotation of the hanging wall of the San Fernando fault about the Pacoima Wash pivot would result in a slip of 6 km at the Sunland segment boundary. The entire surface rupture has been attributed to flexural slip faulting accompanying folding of the Mission Hills and Merrick synclines [*Tsutsumi and Yeats*, 1999]. The sharp bend of the synclinal axes of the Mission Hills and Merrick synclines at the Pacoima segment boundary might be an indication and, possibly, a measure for the rotation of the Merrick syncline domain.

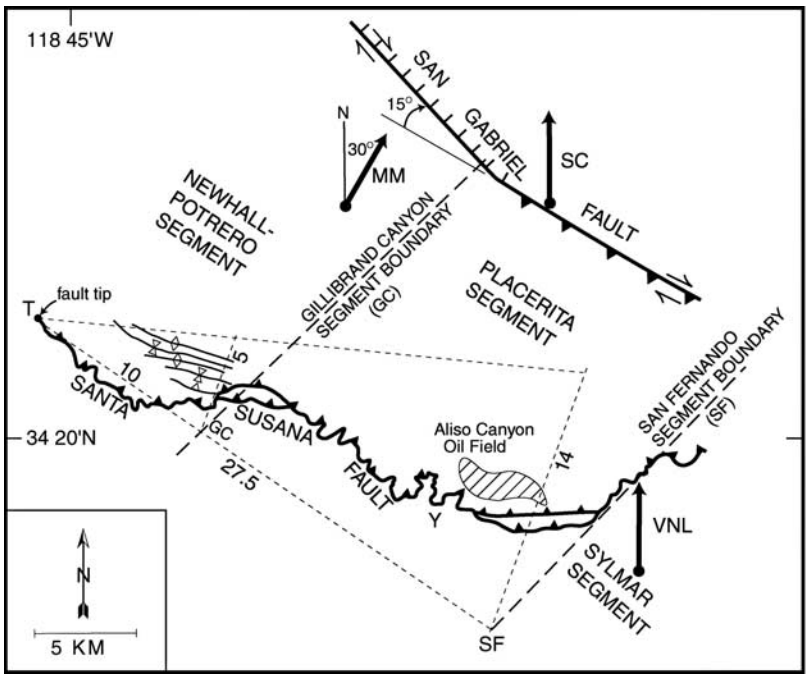

Figure 10. Tectonic map of hanging wall of Santa Susana fault and its relation to the San Gabriel fault. The hanging wall is divided into Newhall-Potrero, Placerita, and Sylmar segments bounded by northeast trending Gillibrand Canyon (GC) and San Fernando (SF) segment boundaries from *Yeats et al.* [1994]. Note 15° bend of San Gabriel fault northeast of GC segment boundary and localized strong folding just west of GC. Declinations of Magic Mountain (MM), Soledad Canyon(SC), and Van Norman Lake (VNL) paleomagnetic sections are shown. Calculations: (1) The entire block, 27.5 km long, rotates about the Santa Susana fault tip (T), producing dip slip displacement at the SF segment boundary of ~14 km; (2) the rotation of a 10 km block (Newhall-Potrero segment) between T and GC results in a displacement of ~5 km.

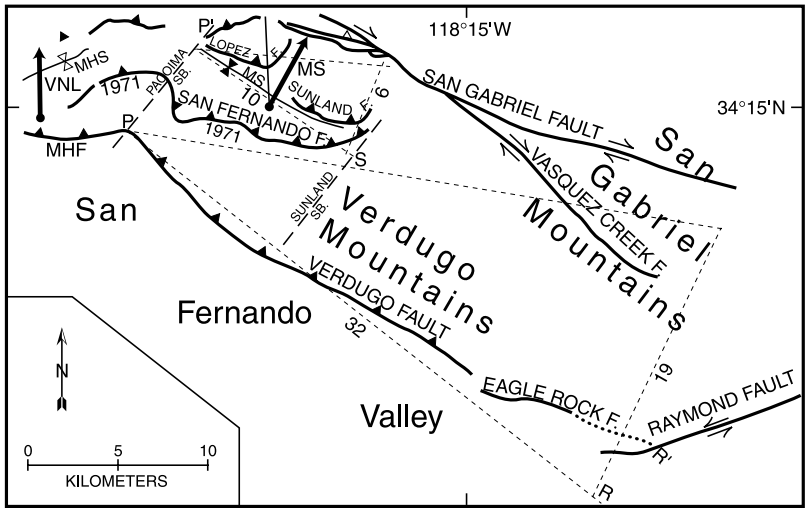

Figure 11. Tectonic map of the area between Mission Hills fault (MHF), Verdugo fault, and Eagle Rock fault on the south and San Gabriel fault on north, showing declinations of Van Norman Lake (VNL) and Merrick syncline (MS) domains. If the 10 km long block between the Pacoima and Sunland segment boundaries in the hanging wall of the San Fernando fault rotates 34° about a pivot in the Pacoima segment boundary, line P–P′, the displacement would be ~6 km. In contrast, if the entire Verdugo Mountains block, 32 km long, rotates about a pivot P at Pacoima Wash, the displacement at R, the intersection of the Eagle Rock and Raymond faults, would be ~19 km, which would require slip rate that far exceeds observations (J. F. Dolan, personal communication, 2002).

The San Fernando fault is preferred as the rotation fault rather than the Verdugo and Eagle Rock faults (Figure 11) for two reasons. First, the geomorphic expression of tectonic activity on the Eagle Rock fault is much more subdued than that of the Verdugo fault (Group C, Southern California Earthquake Center, Active faults in the Los Angeles metropolitan region, http://www.scec.org/research/special, 2001), suggesting that the two faults have different late Quaternary histories. Second, a 34° rotation about a pivot P at Pacoima Wash would produce a 19 km displacement at Raymond fault, which is much greater than the observed present-day displacement rate (J. F. Dolan, personal communication, 2001).

[37] The paleomagnetic observations of Liddicoat are generally consistent with ours; the fragmented domains defined by his data are also associated with reverse fault blocks. The rotated Santa Paula Creek section (number 26, Figure 1) is in the hanging wall of a blind strand of the San Cayetano fault [*Namson and Davis*, 1988; *Huftile and Yeats*, 1995], and the rotated section northwest of Ventura is in the hanging wall of the south dipping Padre Juan fault [*Huftile and Yeats*, 1995].

4.4. Paleolatitudes and Poleward Transport

[38] Tectonic investigations that explore paleolatitudes of terranes depend critically on inclination data to constrain north-south translations. The young age and high-quality paleomagnetic directions of the Saugus Formation are suitable to test empirically the accuracy of the inclinations recorded in this type of continental sediment. Of the four composite sections, only the Magic Mountain domain has an average inclination indistinguishable from that of the geocentric axial dipole at the sampling site [*Levi and Yeats*, 1993]. At the other three domains, Van Norman Lake, Merrick syncline, and Soledad Canyon, the measured inclination shallowing is 6.5°, 6°, and 6°, respectively [*Levi and Yeats*, 1993] (Tables 1 and 2). Inclination flattening in sediments is not uncommon, and it might be caused by imperfect grain alignment during depositon [e.g., *Levi and Banerjee*, 1990], postdepositional compaction [e.g., *Arason and Levi*, 1990; *Kodama and Davi*, 1995], and/or incomplete removal of secondary components of remanence during demagnetization. The measured shallow inclinations in Saugus, in a time interval where north-south transport is small and not resolvable by paleomagnetism, can be considered a 'zero order' estimate on the magnitude of inclination shallowing that must be exceeded before confident conclusions can be advanced concerning transport along lines of longitude.

5. Summary and Conclusions

[39] This study shows that crustal blocks of the eastern WTR have experienced fragmentation and rotations during the Quaternary. While some blocks are unrotated, other domains have undergone rotations of the order of 30° during the past million years, in response to distributed right slip associated with relative motions of the Pacific and North America plates. In the Big Bend of the San Andreas fault, the relative plate motions are more oblique to the fault than they are northwest and southeast of the Big Bend region, with a greater compressive component normal to the San Andreas plate boundary, producing enhanced deformation, crustal thickening, fragmentation, and rotation of small reverse fault blocks (Figure 12). The reverse fault blocks cannot be greater than 10–20 km in linear dimensions; otherwise, the calculated slip rates at their eastern ends would exceed the observed late Quaternary slip rates on these and other faults in the Transverse Ranges (Group C, Southern California Earthquake Center, Active faults in the Los Angeles metropolitan region, http://www.scec.org/research/special, 2001). In the sampling area, observational clues for relative block rotations might be seen in sharp changes in the strike of faults, fault systems and/or fold axes. Tectonic analysis of the eastern part of the WTR must consider ongoing rotations of blocks with dimensions of the order of the thickness of the seismogenic crust.

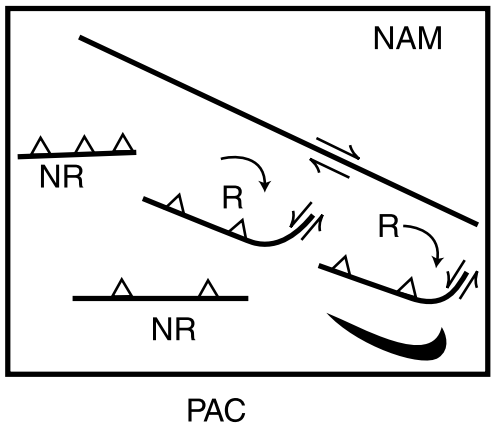

Figure 12. Tectonic model showing the relation between displacement of the Pacific plate (PAC) relative to the North America (NAM) plate at the Big Bend of the San Andreas fault to small-scale hanging wall rotations in the Transverse Ranges to the south. NR, nonrotated fault; R, fault with clockwise rotation, characterized by a straight dip slip section and a left-lateral strike slip section. This makes a boomerang-shaped map pattern, a mirror "swoosh" image.

[40] **Acknowledgments.** We thank Dennis Schultz for assistance in the field and laboratory measurements. This paper benefited from thoughtful and critical reviews by Drs. James Dolan, David Evans, and Bruce Luyendyk. This research was supported by the U. S. Geological Survey (NEHRP contract 14-08-0001-G1353) and the National Science Foundation (EAR-9416324). Further support was received from the Southern California Earthquake Center. SCEC is funded by NSF Cooperative Agreement EAR-0106924 and USGS Cooperative Agreement 02HQAG0008. The SCEC contribution number for this paper is 729.

References

Arason, P., and S. Levi, Compaction and inclination shallowing in deep-sea sediments from the Pacific Ocean, *J. Geophys. Res.*, *95*, 4501–4510, 1990.

Atwater, T., and J. Stock, Pacific-North America plate tectonics of the Neogene southwestern United States: An update, *Intl. Geol. Rev.*, *40*, 375–402, 1998.

Barrows, A. G., J. E. Kahle, R. B. Saul, and F. H. Weber Jr., Geologic map of the San Fernando earthquake area, scale 1:18,000, *Calif. Div. Mines Geol. Bull., 196*, plate 2, 1975.

Beck, M. E., Jr., Discordant paleomagnetic pole positions as evidence of regional shear in the Western Cordillera of North America, *Am. J. Sci.*, *276*, 694–712, 1976.

Beck, M. E., Jr., Paleomagnetic record of plate-margin tectonic processes along the western edge of North America, *J. Geophys. Res.*, *85*, 7115–7131, 1980.

Champion, D. E., D. G. Howell, and M. Marshall, Paleomagnetism of Cretaceous and Eocene strata, San Miguel Island, California, borderland and northward translation of Baja California, *J. Geophys. Res.*, *91*, 11,557–11,570, 1986.

Cloos, E., Experimental analysis of fracture patterns, *Bull. Geol. Soc. Am.*, *66*, 241–256, 1955.

Crouch, J. K., and J. Suppe, Late Cenozoic tectonic evolution of the Los Angeles Basin and inner California borderland: A model for core complex-like crustal extension, *Geol. Soc. Am. Bull.*, *105*, 1415–1434, 1993.

Demarest, H. H., Jr., Error analysis for the determination of tectonic rotation from paleomagnetic data, *J. Geophys. Res.*, *88*, 4321–4328, 1983.

Dibblee, T. W., Jr., Geologic map of the Newhall Quadrangle, *Map DF-56*, scale 1:24,000, Dibblee Geol. Found., Camarillo, Calif., 1996.

Dickinson, W. R., Kinematics of transrotational tectonism in the California Transverse Ranges and its contribution to cumulative slip along the San Andreas transform fault system, *Geol. Soc. Am. Spec. Pap.*, *305*, 46 pp., 1996.

Donnellan, A., B. H. Hager, R. W. King, and T. A. Herring, Geodetic measurement of deformation in the Ventura Basin region, southern California, *J. Geophys. Res.*, *98*, 21,727–21,739, 1993.

Ellis, B. J., S. Levi, and R. S. Yeats, Magnetic stratigraphy of the Morales Formation: Late Neogene clockwise rotation and compression in the Cuyama Basin, California Coast Ranges, *Tectonics*, *12*, 1170–1179, 1993.

Fisher, R., Dispersion on a sphere, *Proc. R. Soc. London, Ser. A*, *217*, 295–305, 1953.

Greenhaus, M. R., and A. Cox, Paleomagnetism of the Morro Rock-Islay Hill complex as evidence for crustal block rotations in central coastal California, *J. Geophys. Res.*, *84*, 2393–2400, 1979.

Hill, M. L., and T. W. Dibblee Jr., San Andreas, Garlock, and Big Pine faults, California, a study of the character, history and tectonic significance of their displacements, *Bull. Geol. Soc. Am.*, *64*, 443–458, 1953.

Hornafius, J. S., Neogene tectonic rotation of the Santa Ynez Range, western Transverse Ranges, California, suggested by paleomagnetic investigation of the Monterey Formation, *J. Geophys. Res.*, *90*, 12,503–12,522, 1985.

Hornafius, J. S., B. P. Luyendyk, R. R. Terres, and M. J. Kamerling, Timing and extent of Neogene tectonic rotation in the western Transverse Ranges, California, *Bull. Geol. Soc. Am.*, *97*, 1476–1497, 1986.

Huftile, G. J., and R. S. Yeats, Convergence rates across a displacement transfer zone in the western Transverse Ranges, Ventura Basin, California, *J. Geophys. Res.*, *100*, 2043–2067, 1995.

Huftile, G. J., and R. S. Yeats, Deformation rates across the Placerita (Northridge $Mw = 6.7$ aftershock zone) and Hopper Canyon segments of the western Transverse Ranges deformation belt, *Bull. Seismol. Soc. Am.*, *86*, S3–S18, 1996.

Jackson, J., and P. Molnar, Active faulting and block rotations in the western Transverse Ranges, California, *J. Geophys. Res.*, *95*, 22,073–22,087, 1990.

Johnson, N. M., C. B. Officer, N. D. Opdyke, G. D. Woodard, P. K. Zeitler, and E. H. Lindsay, Rates of late Cenozoic tectonism in the Vallecito-Fish Creek Basin, western Imperial valley, California, *Geology*, *11*, 664–667, 1983.

Jones, D. L., M. C. Blake, and C. Rangin, The four Jurassic belts of northern California and their significance to the geology of the southern California borderland, *Am. Assoc. Petrol. Geol. Misc. Pap.*, *24*, 343–362, 1976.

Kamerling, M. J., and B. P. Luyendyk, Tectonic rotation of the Santa Monic Mountains in southern California (abstract), *Eos Trans. AGU*, *58*, 1126, 1977.

Kamerling, M. J., and B. P. Luyendyk, Tectonic rotations of the Santa Monica Mountains region, western Transverse Ranges, California, suggested by paleomagnetic vectors, *Geol. Soc. Am. Bull.*, *90*, 331–337, 1979.

Kamerling, M. J., and B. P. Luyendyk, Paleomagnetism and Neogene tectonics of the northern Channel Islands, California, *J. Geophys. Res.*, *90*, 12,485–12,502, 1985.

Kew, W. S. W., Geology and oil resources of a part of Los Angeles and Ventura counties, California, *U.S. Geol. Surv. Bull.*, *753*, 202 pp., 1924.

Khan, S. O., R. S. Coe, and J. A. Barron, Paleomagnetism of the middle-upper Miocene Monterey Formation, Shell Beach, Pismo Basin: Implications for the age and origin of the Monterey and tectonic block rotation in central coastal California, in *Magnetic Stratigraphy of the Pacific Coast Cenozoic*, vol. 91, edited by D. R. Prothero, pp. 302–334, Pacific Section Soc. for Sediment. Geol., Santa Fe Springs, Calif., 2001.

Kodama, K. P., and J. M. Davi, A compaction correction for the paleomagnetism of the Cretaceous Pigeon Point Formation of California, *Tectonics*, *14*, 1153–1164, 1995.

Levi, S., and S. Banerjee, On the origin of inclination shallowing in redeposited sediments, *J. Geophys. Res.*, *95*, 4383–4389, 1990.

Levi, S., and R. S. Yeats, Paleomagnetic constraints on the initiation of uplift on the Santa Susana fault, western Transverse Ranges, California, *Tectonics*, *12*, 688–702, 1993.

Levi, S., D. L. Schultz, R. S. Yeats, L. T. Stitt, and A. M. Sarna-Wojcicki, Magnetostratigraphy and paleomagnetism of the Saugus Formation near Castaic, Los Angeles County, California, in *Field Trip Guidebook and Volume on Neotectonics and Faulting in Southern California and Baja California*, edited by P. E. Ehlig, pp. 103–108, Cordilleran Section Geol. Soc. of Am., Los Angeles, Calif., 1986.

Liddicoat, J. C., Paleomagnetism of the Zuma Volcanics, Point Dume, Los Angeles County, California, *Calif. Geol.*, *41*, 243–247, 1988.

Liddicoat, J. C., Tectonic rotation of the Santa Ynez Range, California, recorded in the Sespe Formation, *Geophys. J. Int.*, *102*, 739–745, 1990.

Liddicoat, J. C., Palaeomagnetism of the Pico Formation, Santa Paula Creek, Ventura County, California, *Geophys. J. Int.*, *110*, 267–275, 1992.

Liddicoat, J. C., Paleomagnetism of the Monterey (Miocene) and Fernando (Pliocene-Pleistocene) formations, Balcom Canyon, Ventura Basin, California, in *Magnetic Stratigraphy of the Pacific Coast Cenozoic*, vol. 91, edited by D. R. Prothero, pp. 335–348, Pacific Section Soc. for Sediment. Geol., Santa Fe Springs, Calif., 2001a.

Liddicoat, J. C., Paleomagnetism of the Fernando Formation (Pliocene-Pleistocene), Ventura Basin, California, in *Magnetic Stratigraphy of the Pacific Coast Cenozoic*, vol. 91, edited by D. R. Prothero, pp. 349–358, Pacific Section Soc. for Sediment. Geol., Santa Fe Springs, Calif., 2001b.

Lonsdale, P., Structural pattern of the Pacific floor offshore of peninsular California, *Am. Assoc. Petrol. Geol. Mem.*, *47*, 87–125, 1991.

Luyendyk, B. P., A model for Neogene crustal rotations, transtension, and transpression in southern California, *Geol. Soc. Am. Bull.*, *103*, 1528–1536, 1991.

Luyendyk, B. P., M. J. Kamerling, R. R. Terres, and J. S. Hornafius, Simple shear of southern California during the Neogene time suggested by paleomagnetic declinations, *J. Geophys. Res.*, *90*, 12,454–12,466, 1985.

McDougall, I., The present status of the geomagnetic polarity time scale, in *The Earth: Its Origin, Structure and Evolution*, edited by M. W. McElhinny, 543 pp., Academic, San Diego, Calif., 1979.

McDougall, I., F. H. Brown, T. E. Cerling, and J. W. Hillhouse, A reappraisal of the geomagnetic polarity time scale to 4 Ma using data from the Turkana Basin, east Africa, *Geophys. Res. Lett.*, *19*, 2349–2352, 1992.

Molnar, P., and J. M. Gipson, Very long baseline interferometry and active rotations of crustal blocks in the western Transverse Ranges, California, *Bull. Geol. Soc. Am.*, *106*, 594–606, 1994.

Namson, J., and T. Davis, Structural transect of the western Transverse Ranges, California: Implications for lithospheric kinematics and seismic risk evaluation, *Geology*, *16*, 675–679, 1988.

Ness, G. E., M. W. Lyle, and R. W. Couch, Marine magnetic anomalies and oceanic crustal isochrons of the Gulf and Peninsular Province of the Californias, *Am. Assoc. Petrol. Geol. Mem.*, *47*, 87–125, 1991.

Nicholson, C., C. C. Sorlien, T. Atwater, J. C. Crowell, and B. P. Luyendyk, Microplate capture, rotation of the western Transverse Ranges, and initiation of the San Andreas transform as a low-angle fault system, *Geology*, *22*, 491–495, 1994.

Oakeshott, G. B., Geology and mineral deposits of San Fernando Quadrangle, Los Angeles County, California, *Calif. Div. Mines Bull.*, *172*, 147 pp., 1958.

Prothero, D. R., and J. R. Britt, Magnetic stratigraphy and tectonic rotation of the Middle Eocene Matilija Sandstone and Cozy Dell Shale, Ventura County, California: Implications for sequence stratigraphic correlations, *Earth Planet. Sci. Lett.*, *163*, 261–273, 1998.

Prothero, D. R., and J. Hoffman, Magnetic stratigraphy of upper Oligocene-lower Miocene Soda Lake Shale Member of the Vaqueros Formation, Caliente Range, San Luis Obispo County, California, in *Magnetic Stratigraphy of the Pacific Coast Cenozoic*, vol. 91, edited by D. R. Prothero, pp. 254–263, Pacific Section Soc. for Sediment. Geol., Santa Fe Springs, Calif., 2001.

Prothero, D. R., and S. G. Rapp, Magnetic stratigraphy and tectonic rotation of the lower Miocene (type Saucesian) Rincon Formation, Ventura and Santa Barbara Counties, California, in *Magnetic Stratigraphy of the Pacific Coast Cenozoic*, vol. 91, edited by D. R. Prothero, pp. 263–271, Pacific Section Soc. for Sediment. Geol., Santa Fe Springs, Calif., 2001.

Prothero, D. R., and R. B. Vacca, Magnetic stratigraphy and tectonic rotation of the upper Paleocene Pattiway Formation, Caliente Range, San Luis Obispo County, California, in *Magnetic Stratigraphy of the Pacific Coast Cenozoic*, vol. 91, edited by D. R. Prothero, pp. 20–26, Pacific Section Soc. for Sediment. Geol., Santa Fe Springs, Calif., 2001.

Ricketts, E. W., and K. R. Whaley, Structure and stratigraphy of the Oak Ridge fault-Santa Susana fault intersection, Ventura Basin, California, M.S. thesis, 81 pp., Ohio Univ., Athens, 1975.

Sharp, R. V., Displacement on tectonic ruptures, in San Fernando, California, earthquake of 9 February 1971, *Calif. Div. Mines Geol. Bull.*, *196*, 187–194, 1975.

Singer, B. S., K. A. Hoffman, A. Chauvin, R. S. Coe, and M. S. Pringle, Dating transitionally magnetized lavas of the late Matuyama Chron: Toward a new $^{40}Ar/^{39}Ar$ timescale of reversals and events, *J. Geophys. Res.*, *104*, 679–693, 1999.

Swanson, B. J., Geologic investigation of a portion of the San Gabriel fault southeast of Bouquet Junction, City of Santa Clarita, southern California, in *Geology and Tectonics of the San Fernando Valley and East Ventura Basin, California: Pacific Section American Association of Petroleum Geologists Guidebook*, vol. 77, edited by T. L. Wright and R. S. Yeats, pp. 91–104, Pac. Sect. Am. Assoc. Petrol. Geol., Bakersfield, Calif., 2001.

Teissere, R. F., and M. E. Beck Jr., Divergent Cretaceous paleomagnetic pole position for the southern California Batholith, U.S.A., *Earth Planet. Sci. Lett.*, *18*, 297–300, 1973.

Terres, R. R., and B. P. Luyendyk, Neogene tectonic rotation of the San Gabriel region, California, suggested by paleomagnetic vectors, *J. Geophys. Res.*, *90*, 12,467–12,484, 1985.

Tsutsumi, H., and R. S. Yeats, Tectonic setting of the 1971 Sylmar and 1994 Northridge earthquakes in the San Fernando valley, California, *Bull. Seismol. Soc. Am.*, *89*, 1232–1249, 1999.

Whidden, K. J., S. P. Lund, and D. J. Bottjer, Extension of the western Transverse Ranges zone of Cenozoic block rotations north of the Santa Ynez fault, California, in *Cenozoic Paleogeography of the Western United States-II*, vol. 75, edited by A. E. Fritsche, pp. 181–192, Pacific Section Soc. for Sediment. Geol., Fullerton, Calif., 1995.

Whitcomb, J. H., C. R. Allen, J. D. Garmany, and J. A. Hileman, San Fernando earthquake series, 1971: Focal mechanisms and tectonics, *Rev. Geophys.*, *11*, 693–730, 1973.

Winterer, E. L., and D. L. Durham, Geology of southeastern Ventura Basin, Los Angeles County, California, *U.S. Geol. Surv. Prof. Pap.*, *334-H*, 275–366, 1962.

Yeats, R. S., Late Cenozoic structure of the Santa Susana fault zone, *U.S. Geol. Surv. Prof. Pap.*, *1339*, 161–167, 1987.

Yeats, R. S., and L. T. Stitt, Ridge Basin and San Gabriel fault in the Castaic lowland, southern California, *Geol. Soc. Am. Spec. Pap.*, *367*, 121–156, 2003.

Yeats, R. S., G. J. Huftile, and L. T. Stitt, Late Cenozoic tectonics of the east Ventura Basin, Transverse Ranges, California, *AAPG Bull.*, *78*, 1040–1074, 1994.

S. Levi, College of Oceanographic and Atmospheric Sciences, Oregon State University, Corvallis, OR 97331, USA. (slevi@oce.orst.edu)

R. S. Yeats, Department of Geosciences, Oregon State University, Corvallis, OR 97331, USA. (yeatsr@science.oregonstate.edu)